Available online at www.sciencedirect.com
ScienceDirect
Journal of Power Sources 162 (2006) 1416–1420
JOURNAL OF POWER SOURCES
www.elsevier.com/locate/jpowsour

Short communication

Characteristics and performance of 10 kW class all-vanadium redox-flow battery stack

Ping Zhao *, Huamin Zhang **, Hantao Zhou, Jian Chen, Sujun Gao, Baolian Yi

PEMFC Key Materials & Technology Laboratory, Dalian Institute of Chemical Physics (DICP), Chinese Academy of Sciences, Dalian, Liaoning 116023, PR China

Received 25 July 2006; accepted 10 August 2006
Available online 20 September 2006

Abstract

A kW class all-vanadium redox-flow battery (VRB) stack, which was composed of 14 cells each with an electrode geometric surface area of 875 cm^2, with an average output power of 1.14 kW, at the charge–discharge current density of 70 mA cm^{-2}, was successfully assembled by filter press type. Then, a 10 kW class VRB stack was manufactured with a configuration of 4 × 2 (serial × parallel) of the improved aforementioned kW class stack modules, which produced a direct output of 10.05 kW (current density 85 mA cm^{-2}). The energy efficiency of more than 80%, at an average output power of 10.05 kW, for the 10 kW class VRB stack was achieved, indicating VRB is a promising high efficiency technology for electric storage.

Keywords: Vanadium redox-flow battery; Energy storage; Cell stack

1. Introduction

For a sustainable and clean future, considerations are increasingly given to the limitless renewable energy such as solar, wind, wave, etc. It can be anticipated that renewable power sources will make increasing contributions to electricity generation in the decades ahead [1]. Renewables, however, possess the variable and intermittent nature of their output, so there is often the problem of matching the supply to meet the demand [1]. To make better use of the electricity generated by renewables, research, development and application of economical and efficient energy-storage systems become indispensable and urgent [1]. Of all the new energy storage technologies currently under development around the world, the redox flow battery (RFB) appears to offer great promise as a low cost, high-efficiency large-scale energy storage system [2–8] and has been reviewed recently [9].

All-vanadium redox flow battery (VRB) proposed by Skyllas-Kazacos et al. [4–6] holds all the merits of other RFBs [2,3]. Moreover, because of using only vanadium species for both halves of the cell, the problem of electrolytes cross-contamination through battery separator was overcome [4–6]. Based on these attractive features, more and more attentions have been paid to VRB recently [7–18].

In 1991, a VRB cell stack was fabricated by Skyllas-Kazacos et al., which produced an average power output of 1.1 kW at the discharge current density of 60 mA cm^{-2} with an energy efficiency of 77.7% [5].

Different kinds of RFBs have been studied at our research group since 1989 [3,17–26]. In this work, we focused on the characteristics and performance of the VRB cell stack recently developed in our lab.

2. Principle of VRB

As shown in Fig. 1, the VRB has two electrolyte loops both containing vanadium in sulfuric acid medium, but in different valence states which may be oxidized/reduced at the electrodes. The vanadium redox pairs are V^{2+}/V^{3+} and V^{4+}/V^{5+} for negative and positive halves of the cell, respectively. The electrical balance is achieved by the transport of hydrogen ions in the electrolytes across the membrane during operation of the cell.

* Corresponding author. Tel.: +86 411 84379535; fax: +86 411 84665057.
** Co-corresponding author.
E-mail addresses: zp567@dicp.ac.cn (P. Zhao), zhanghm@dicp.ac.cn (H. Zhang).

0378-7753/$ – see front matter © 2006 Elsevier B.V. All rights reserved.
doi:10.1016/j.jpowsour.2006.08.016

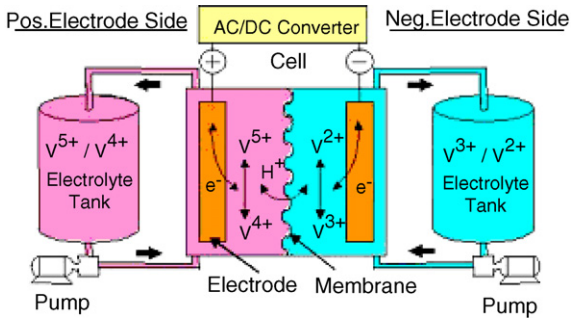

Fig. 1. Operation principle of the VRB flow single cell. Positive electrode side: $V^{4+} - e \underset{\text{discharge}}{\overset{\text{charge}}{\rightleftharpoons}} V^{5+}$; negative electrode side: $V^{3+} + e \underset{\text{discharge}}{\overset{\text{charge}}{\rightleftharpoons}} V^{2+}$. Photo courtesy of Sumitomo Electric Industries Ltd. (SEI). Copyright 2001.

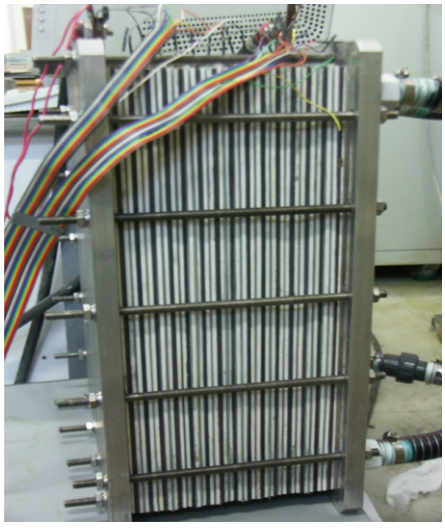

Fig. 2. Photo of 14-cell 1 kW class VRB cell stack. Single cell index: 1 → 14.

3. Experimental

The 1 kW class VRB cell stack, as shown in Fig. 2, was constructed according to the specifications given in Table 1.

The carbon felt (Shanghai XinXing Carbon Co. Ltd., China) was chemically treated before being used as the negative and positive electrode materials for VRB.

The charge–discharge cycle test was conducted by Arbin Instrument (Model BT 2000, Arbin Instruments Corp., USA), which ran under the control of presetting schedules given by us. The stack coulombic efficiency (CE) is defined as the discharge capacity (Ah) divided by the charge capacity, energy efficiency (EE) as discharge energy (Wh) divided by charge energy. Then the voltage efficiency (VE) can be calculated from VE = EE/CE. All the data of the charge/discharge capacity and energy were recorded by Arbin instrument automatically.

Table 1
Specifications for 1 kW class VRB stack

Area of felt electrode	875 cm^2
Number of cells	14
Membrane material	Nafion (Du Pont)
Bipolar electrode material	Graphite plate
Material of electrode frame	PVC (polyvinyl chloride)
Material of end plate	Aluminum alloy
Stack dimensions ($L \times W \times H$)	440 mm × 340 mm × 200 mm
Electrolyte	1.5 M $VOSO_4$ + 3 M H_2SO_4
Electrolyte volume per half-cell/l	7.4
Operate temperature	Ambient

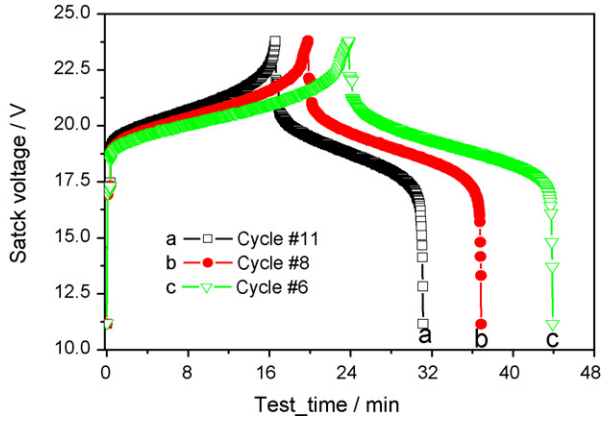

Fig. 3. Charge–discharge curves for 1 kW class VRB cell stack at current density of (a) 70 mA cm^{-2}, (b) 60 mA cm^{-2}, and (c) 50 mA cm^{-2}.

4. Results and discussion

4.1. Performance of 14-cell 1 kW VRB stack

The CE of the stack increases with the increasing of the current density, as can be seen from Table 2. This phenomenon could be attributed to that with the increasing of the current density, the charge and discharge cycle time become shorter (see Fig. 3), thus lowering the diffusion of the electrochemical active species through the membrane, and hence the rate of self-discharge of the cell. However, the overall polarization of the stack could become larger unavoidably, with the increasing of the current density, thus a decreasing of VE can be expected. The change

Table 2
Performance of 1 kW class VRB stack

Cycle index	Charge–discharge current (A)	Current density (mA cm^{-2})	Average output voltage (V)	Average output power (kW)	CE (%)	VE (%)	EE (%)
1st	74.38	85	18.19	1.353	–	–	–
2–4th	34.97	40	19.10	0.668	82.62	93.64	77.37
5–7th	43.72	50	19.07	0.834	84.00	92.49	77.73
8–9th	52.46	60	18.88	0.991	85.90	91.10	78.25
10–11th	61.23	70	18.68	1.144	87.12	89.68	78.12

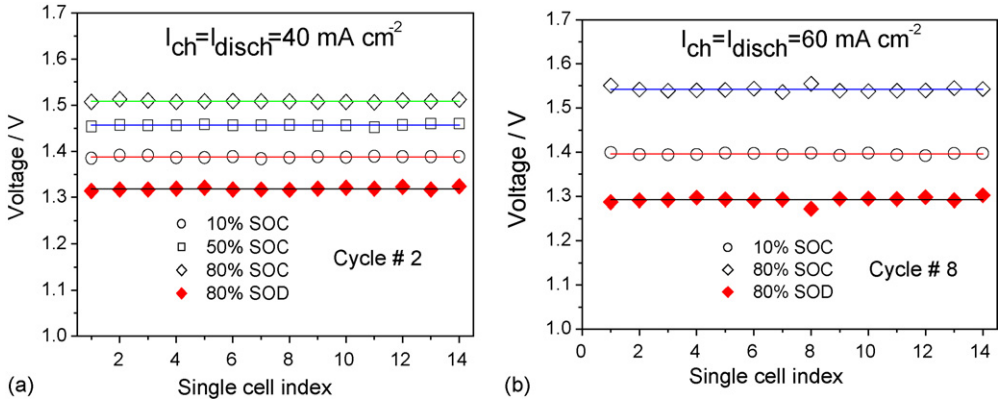

Fig. 4. Distribution of voltage in the 14-cell 1 kW VRB stack.

of EE is subjected to that of CE and VE, since EE = CE × VE. From Table 2, it can be seen that the coulombic, voltage and energy efficiency was up to 85.9%, 91.1% and 78.3%, respectively, at a current density of 60 mA cm^{-2}, and a maximum average output power of 1.35 kW at a discharge current density of 85 mA cm^{-2} was determined. Comparison with the performance data reported in Ref. [5], the stack in this work possesses higher VE and EE, but a lower CE at the same charge–discharge current density, indicating that the internal resistance (IR) drop and electrochemical polarization of electrode reactions during the operation of the stack are lower. However, the lower CE of the stack implied that the stack at this stage needs further optimizing [27].

4.2. Voltage distribution in the 14-cell 1 kW VRB stack

In a RFB cell stack assembled by filter press type, uniform performance of each unit cell is of great importance. Fig. 4 exhibits the voltage distribution of the stack at various state-of-charge (SOC), state-of-discharge (SOD) and charge–discharge current densities, revealing that voltage distribution in the stack was extraordinarily uniform, especially at lower SOC or SOD and current density, which indicates fairly uniform distribution of the IR, the reactant electrolytes from the electrolyte inlet to the outlet and activation polarization of the electrodes of unit cells in the stack. The cell index was designated as in Fig. 2. The standard deviation of the unit cell voltages was 2.14, 5.20, and 6.84 mV at the SOC of 10%, 80% and SOD of 80% and a charge–discharge current density of 60 mA cm^{-2}, as presented in Fig. 4(b), respectively.

4.3. Fabrication and performance of 10 kW class VRB cell stack

Based on the results given by 14-cell 1 kW class VRB stack, a 10 kW VRB stack system was constructed with a configuration of 4 × 2 (serial × parallel) of the improved aforementioned kW class stack modules, as presented in Fig. 5.

Comparing the performance of 10 kW class VRB stack summarized in Table 3 with that of 1 kW class stack in Table 2, it is clear that the CE of 10 kW class stack in Table 3 is much higher than that of 1 kW stack in Table 2, indicating the measures employed to modify the 1 kW class VRB stack are effective to reduce the shunt current [26,27], hence, increase the CE of the stack. A maximum in the overall EE of up to 82.4% is observed at a current density of 50 mA cm^{-2}. The CE, VE and EE of the stack is 92.9%, 86.5% and 80.4%, respectively, and the output power is 10.05 kW at a discharge current density of 85 mA cm^{-2}, as shown in Table 3.

In order to study the influence of module configuration on output power, the stack power–discharge current density curves of VRB stack with configurations of 4S × 2P (serial × parallel)

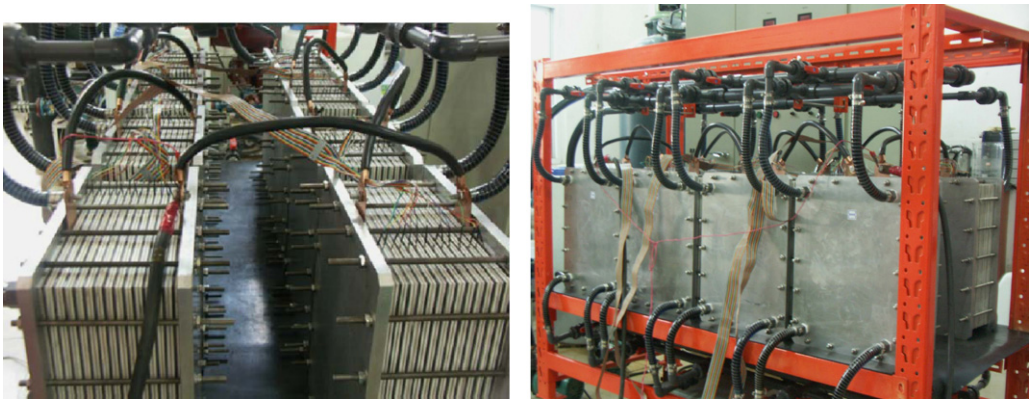

Fig. 5. Photos of 10 kW class VRB cell stack composed of eight 1 kW stack modules with a configuration of 4 × 2 (serial × parallel).

Table 3
Performance of 10 kW class VRB cell stack

Charge–discharge current (A)	Charge–discharge current density (mA cm^{-2})	Average output power (kW)	CE (%)	VE (%)	EE (%)
C105–D149	C60–D85	10.05	92.94	86.54	80.43
C105–D140	C60–D80	9.53	92.03	87.19	80.24
122.5	70	8.41	93.03	87.06	80.99
105	60	7.23	91.77	88.20	80.94
87.5	50	6.14	90.95	90.54	82.35
70	40	4.95	89.02	92.03	81.93

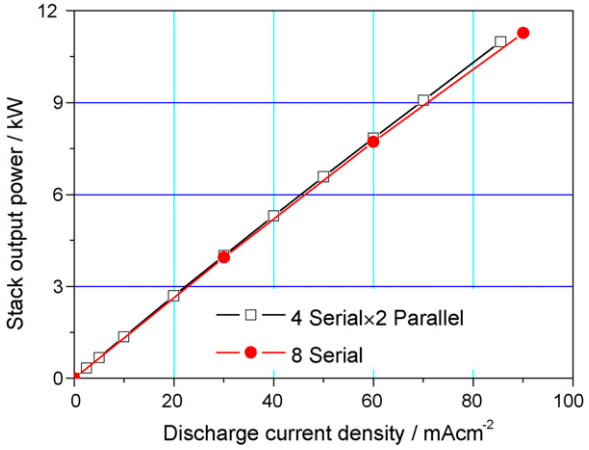

Fig. 6. Power–current density curves for eight-module 10 kW class VRB stack with different configurations of kW class stack modules.

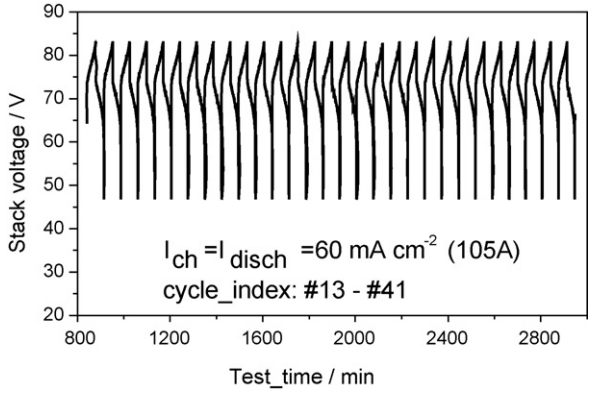

Fig. 8. Charge–discharge cyclic curves of VRB stack.

and 8S (serial) were determined, respectively, and illustrated in Fig. 6. The little difference in output power of 10 kW VRB stack with various configurations, as shown in Fig. 6, tells us that the module configuration has nearly no influence on the output power of the stack, indicating the scale-up of VRB stack can be easily by serial and/or parallel connection of stack modules to increase the output voltage and/or current, hence the output power. The output power of 11.3 kW (power density is ca. 0.13 W cm^{-2}) is achieved, as can be seen from Fig. 6, at the current density of 90 mA cm^{-2}. The true peak power of this stack has not yet been established, however, due to equipment limitations.

Fig. 7 shows the voltage distribution of the 10 kW class VRB stack at various SOC, SOD and current densities, revealing that voltage distribution in the stack was fairly uniform, and a little influence of scale-up from 1 kW stack to 10 kW one on the uniform distribution of the internal resistance (IR), the electrochemically active solutions and polarization of the electrodes of unit cells in the stack. The standard deviation of the unit cell voltages was 5.78, 8.94, and 8.12 mV at the SOC of 10% and 80% and SOD of 80% in Fig. 7(a), respectively.

A series of uninterrupted charge–discharge curves obtained at the current density of 60 mA cm^{-2} is given in Fig. 8, which is fairly smooth, revealing that the cyclic performance of the stack is excellent. Fig. 9 shows a plot of coulombic, voltage and energy efficiency as a function of cycle number corresponding to Fig. 8. The average values of CE, VE and EE of the stack illustrated in Fig. 9 are about 91.8%, 88.2% and 80.9%, respectively.

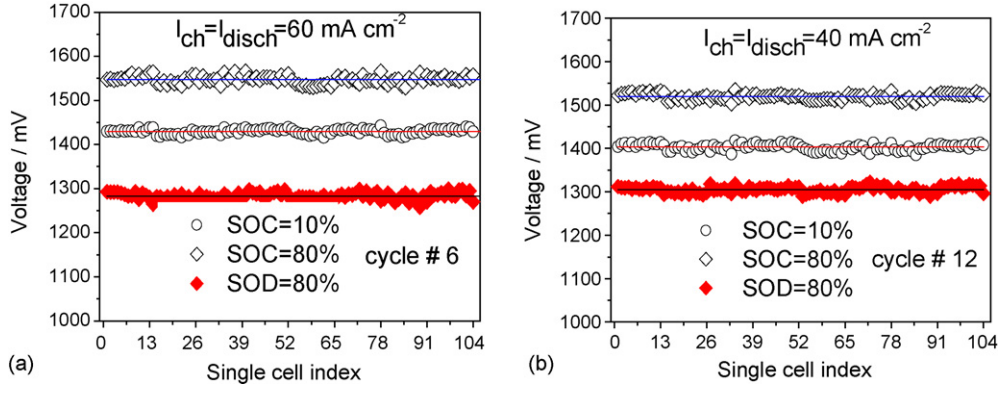

Fig. 7. Distribution of voltage in the eight-module 10 kW class VRB stack at various current density.

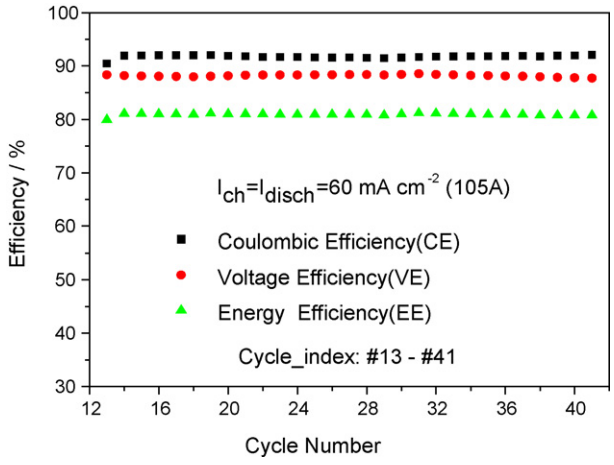

Fig. 9. Coulombic, voltage and energy efficiencies of 10 kW class VRB stack.

5. Conclusions

A 14-cell 1 kW class VRB stack was established and the performance of the stack was studied. Then, a 10 kW class VRB stack with a configuration of 4×2 (serial $\times$ parallel) of the modified kW class stack modules was successfully fabricated in this work. The eight-module 10 kW VRB stack exhibited excellent cyclic performance and stability of efficiency. A maximum energy efficiency of 82.35% for the 10 kW stack at the charge–discharge current density of 50 mA cm^{-2} was obtained. The research and development of 5 kW and more VRB stack module, novel bipolar plate, high electrochemical activation electrode material and low cost high performance ion exchange membrane are now in progress at our lab, which will be reported in the near future.

Acknowledgement

This work is supported by the national 863 program of China (Grant no. 2005AA516020).

References

[1] R.M. Dell, D.A.J. Rand, J. Power Sources 100 (2001) 2.
[2] L.H. Thaller, US Patent 3,996,064 (1976).
[3] P. Zhao, H. Zhang, H. Zhou, B. Yi, Electrochim. Acta 51 (2005) 1091.
[4] M. Skyllas-Kazacos, M. Rychcik, R.G. Robins, A.G. Fane, M.A. Green, J. Electrochem. Soc. 133 (1986) 1057.
[5] M. Skyllas-Kazacos, D. Kasherman, D.R. Hong, M. Kazacos, J. Power Sources 35 (1991) 399.
[6] H. Vafiadis, M. Skyllas-Kazacos, J. Membr. Sci. 279 (2006) 394.
[7] A. Shibata, K. Sato, Power Eng. J. 13 (1999) 130.
[8] L. Joerissen, J. Garche, Ch. Fabjan, G. Tomazic, J. Power Sources 127 (2004) 98.
[9] C. Ponce de León, A. Frías-Ferrer, J. González-García, D.A. Szánto, F.C. Walsh, Redox flow cells for energy conversion, J. Power Sources 160 (2006) 716–732.
[10] G. Oriji, Y. Katayama, T. Miura, Electrochim. Acta 49 (2004) 3091.
[11] B. Tian, C.-W. Yan, F.-H. Wang, J. Appl. Electrochem. 34 (2004) 1205.
[12] T. Sukkar, M. Skyllas-Kazacos, J. Appl. Electrochem. 34 (2004) 137.
[13] B. Tian, C.W. Yan, F.H. Wang, J. Membr. Sci. 234 (2004) 51.
[14] M. Gattrell, J. Qian, C. Stewart, P. Graham, B. MacDougall, Electrochim. Acta 51 (2005) 395.
[15] G. Oriji, Y. Katayama, T. Miura, J. Power Sources 139 (2005) 321.
[16] X. Luo, Z. Lu, J. Xi, Z. Wu, W. Zhu, L. Chen, X. Qiu, J. Phys. Chem. B 109 (2005) 20310.
[17] Y. Wen, H. Zhang, P. Qian, P. Zhao, H. Zhou, B. Yi, Acta Phys.-Chim. Sin. 22 (2006) 403.
[18] P. Zhao, H. Zhang, H. Zhou, B. Yi, Chin. J. Power Sources 30 (2006) 141 (in Chinese).
[19] B. Yi, B. Liang, E. Zhang, L. Wu, J. Chem. Ind. Eng. (China) 43 (1992) 330 (in Chinese).
[20] S.H. Ge, B.L. Yi, H.M. Zhang, J. Appl. Electrochem. 34 (2004) 181.
[21] H. Zhou, H. Zhang, P. Zhao, B. Yi, Electrochemistry 74 (2006) 296.
[22] S. Ge, B. Yi, Y. Fu, H. Liu, H. Zhang, Chin. J. Power Sources 26 (2002) 355 (in Chinese).
[23] H. Zhou, H. Zhang, P. Zhao, B. Yi, Electrochim. Acta 51 (2006) 6304.
[24] Y.H. Wen, H.M. Zhang, P. Qian, H.T. Zhou, P. Zhao, B.L. Yi, Y.S. Yang, Electrochim. Acta 51 (2006) 3769.
[25] Y.H. Wen, H.M. Zhang, P. Qian, H.T. Zhou, P. Zhao, B.L. Yi, Y.S. Yang, J. Electrochem. Soc. 153 (2006) A929.
[26] H. Zhang, H. Zhou, P. Zhao, S. Gao, J. Chen, B. Yi. Chinese Patent, Application No. CN200610046183.6 (2006).
[27] G. Codina, A. Aldaz, J. Appl. Electrochem. 22 (1992) 668.